

ChemComm

Accepted Manuscript



This is an *Accepted Manuscript*, which has been through the Royal Society of Chemistry peer review process and has been accepted for publication.

Accepted Manuscripts are published online shortly after acceptance, before technical editing, formatting and proof reading. Using this free service, authors can make their results available to the community, in citable form, before we publish the edited article. We will replace this *Accepted Manuscript* with the edited and formatted *Advance Article* as soon as it is available.

You can find more information about *Accepted Manuscripts* in the [Information for Authors](#).

Please note that technical editing may introduce minor changes to the text and/or graphics, which may alter content. The journal's standard [Terms & Conditions](#) and the [Ethical guidelines](#) still apply. In no event shall the Royal Society of Chemistry be held responsible for any errors or omissions in this *Accepted Manuscript* or any consequences arising from the use of any information it contains.



COMMUNICATION

Fluorescence Imaging Technology (FI) for High-Throughput Screening of Selenide-Modified Nano-TiO₂ Catalysts

Liping Wang, Jianchao Lee^a, Meijuan Zhang, Qiannan Duan, Jiarui Zhang, Hailang Qi
Lab of Env-Mat, Department of Environmental Science, Shaanxi Normal University, Xi'an 710062, China

Received 00th January 20xx,
Accepted 00th January 20xx

DOI: 10.1039/x0xx00000x

A high-throughput screening (HTS) method based on fluorescence imaging (FI) was implemented firstly to evaluate catalytic performance of selenide-modified nano-TiO₂. Chemical ink-jet printing (IJP) technology was reformed to fabricate a catalyst library comprising 1405 (Ni_aCu_bCd_cCe_dIn_eY_f)Se_x/TiO₂ (M₆Se/Ti) composite photocatalysts. Nineteen M₆Se/Tis were screened out from the 1405 candidates efficiently.

Photocatalysis has been studied extensively as a promising environmental remediation technology for removal of contaminants.¹⁻³ Nano-TiO₂ photocatalysts applied in the fields of water splitting, organic degradation have obtained much more achievements.^{4,5} While there were still many limits in the development of these catalysts.⁶ Doping or modifying pure nano-TiO₂ photocatalyst to promote its photocatalytic activity become an urgent task, which is also benefit for the popularization and application of heterogeneous photocatalytic technology.⁷⁻⁹

Among all the technologies for improving the photocatalytic activity of nano-TiO₂, composite semiconductor modification has attracted much more attention. There were a variety of the materials or their mixtures being synthesized as catalysts.¹⁰⁻¹² Conventionally, when researchers chose the co-semiconductor, they have to carry experiments based on the existing records or inexact concludes. Consuming lots of manpower and resources, they did screening, optimization, and verification repeatedly, while got little substantial progress.^{1, 13} The recent emergence of high-throughput screening technology has fundamentally changed people's thinking mode because of its efficient, sensitive characters and performance of being a one-time detection of large samples. As an alternative pathway, appropriate high-throughput screening technologies are apt to overcome the obstacle and to broaden the sight of researchers.¹⁴⁻¹⁶ HTS method is opening a promising method for highly efficient discovery and optimization of new catalysts.^{22, 28}

The selenides of Ni, Cu, Cd, Ce, In or Y had been reported extensively as photocatalyst materials, exhibiting good photocatalytic performance.²³⁻²⁷ We choose selenide-modified TiO₂ nano-

particle as target photocatalysts. In view of the above mentioned investigations, we are in an attempt to confirm the applicability of a new HTS method for determining the photocatalytic performance of selenide-modified TiO₂. In our work, for evaluation of photocatalytic performance of the prepared catalysts, the aqueous eosin (detailed formula and spectrum in supporting information Figure S6) degradation is chosen as the target reaction. UV-lithography technology will be adopted and adjusted to prepare chips containing numerous independent microreactors. A composite catalyst library M₆Se/Ti will be established by a reformed IJP method. For its advantages of high stability, sensitivity and efficiency, fluorescence imaging (FI) is selected to evaluate the catalytic performance of the catalysts in all react units (denoted clearly as react-unit).

At the initial stage, a new microreactor chip (denoted as MR-chip) of HTS experiment was fabricated by UV-lithography technique.^{29, 30} The obtained MR-chip was comprised of thousands of tiny cells (500 × 500 μm), with a structure of hydrophobic border and hydrophilic cell (Figure S1b). The typical operation was schematically depicted in Figure S1 (See Supporting Information for details). The prepared MR-chip possessed some features. The measurements of the contact angles of the material surface (Figure S2) revealed the glass substrate was highly hydrophilic and the calcined PVL surface was super hydrophobic. The photos of aqueous solution in the cells (Figure S1c) displayed the water was well separated by the grid lines and stabilized into the grid cells. These direct tests confirmed the well implementation of the independent microreactors on MR-chip.

The establishment of catalyst libraries was fulfilled by means of chemical printing, i.e. IJP technology^{31, 32}. It can be used to construct catalyst libraries with controlling the proportions and placements of precursor solutions. A designed navigation template (Figure 1a) was comprised of two layers. Regular CMY values were at all points in each layer, representing ink quantities of cyan, magenta, and yellow (CMY). These three inks were corresponded to three metal solutions. Amounts and location of the metal solutions were controlled by tuning the output of these three inks (between 0-100% in steps of 1%). The intensity of the color directly reflected the concentration of the printed 'ink'. CMY values are continuous and variable in the template. Based on the above template, a library of 1405 M₆Se/Ti (M = Ni, Cu, Cd,

^ajianchaolee@snnu.edu.cn

Electronic Supplementary Information (ESI) available: Detailed experimental sections, Figure S1–S5 and Supplementary Table S1–S3. See DOI: 10.1039/x0xx00000x

Ce, In, Y) was realized in a printing area (enclosed in Figure 1b, denoted as PA). The gray value of the designed template (Figure S3) was in statistic to reflect the variation of CMY values. In the gray variation of a strip (Figure 1a) there was a regular and continuous gray value, implying diverse proportions of printing metals.

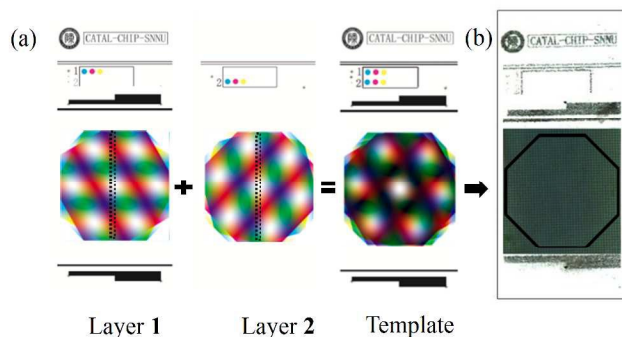


Figure 1. (a) the designed template and (b) the as-printed MR-chip following the template.

For the printing inks, a series of metal precursor solutions were prepared. Particularly, surface tension was adjusted with ethanol and ethylene glycol monobutyl ether to make it exactly consistent with original ink, ensuring the proper run of printer. Prior to printing step, some prepared pure TiO_2 nanoparticle (~ 25 nm) was transplanted into the cells on MR-chip elaborately. In the operation, the nano- TiO_2 (100 mg) was dispersed in 10 ml ethylene glycol solution (10 vol%) with the aid of sonication. Then the suspension was quantitatively sprayed on a MR-chip evenly by an airbrush (See Supporting Information for details).

IJP technology was reformed to fabricate composite catalysts library. Here, we employed a commercial color ink-jet printer (Lenovo 3110) to complete the job. For the overprint actions on the glass slide accurately, the transmission system of the printer was completely reformed. The printing process was described in Supporting Information for details. With the guide of the designed templates (Figure 1), 6 metal solutions were printed on MR-chip as precursors. The 1405 CMY values and specific metal atomic ratios (R_{atom}) of $\text{M}_6\text{Se/Ti}$ catalysts in all react-units were displayed in Table S2. After printing operation, a gas-phase selenizing process in an autoclave was adopted to obtain the target catalyst library (See Supporting Information for details).

Some experiments of catalyst characterization were carried out to ascertain whether the as-prepared catalysts were consistent with the preset printing values. Randomly, the catalyst in a unit (located at (0.32, 0.79), the red square on Figure S4c) were selected as an example. From the EDS spectra of the composite catalyst (Figure S4), the R_{atom} was 0.16:0.02:0.11:0.53:0.00:0.18 of the 6 metals (Ni, Cu, Cd, Ce, In, Y). While the ratio was 0.17:0.01:0.12:0.51:0.00:0.19 calculated from the preset printing values. With a relative error $\leq 6\%$, the prepared catalyst followed the intended components.

The eosin photocatalytic degradation was carried out in a novel 2D reactor designed for our HTS experiment specifically. The reactor was composed of a quartz glass window, a silica circle, as-prepared MR-chip and a glass baseplate (Figure 2). The assembled reactor formed a confined space with a height of only hundreds of microns. The confined space effectively avoided the evaporation of the solution, being confirmed in our previous research.³³ During running, certain amount of substrate solution (aqueous eosin, 1 g/L) was atomized into microdroplets (size: 1

to 5 μm) by an ultrasonic nebulizer firstly, and then fell on the surface of MR-chip. Owing to the hydrophobicity of the grid lines, the microdroplets were finally dispersed and stood in the cells, ensuring the independence of each react-unit. The assembled reactor was stabilized in dark for 30 min. Then the reactor was running under irradiation of 365-nm UV. Simultaneously, a CCD camera was utilized to capture fluorescent images of the PA in a certain time interval to record the change of fluorescence intensity (I^f) in all units.

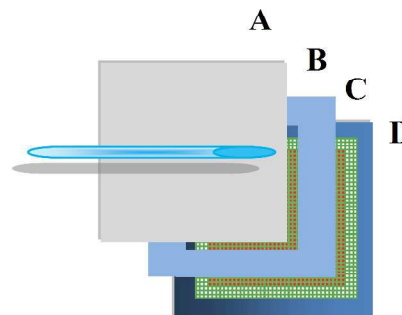


Figure 2. An airtight 2D reactor made up of (A) quartz glass window, (B) silica circle, (C) as-prepared MR-chip and (D) glass baseplate.

Fluorescence images (Figure 3) were captured to evaluate the catalytic performance of catalysts on MR-chip. In the process of eosin degradation, I^f decreased with the concentration of fluorogenic substrate. Because of the performance of varied components of catalysts, react-units displayed diverse I^f changes. Some luminous spots at initial time were darkening following the 40 min photoreaction in the PA, which indicates that the catalysts' activity is higher in this area. The detailed I^f of every react-unit was a database, which is rich resource to explore numerous aspects of catalysts performance.

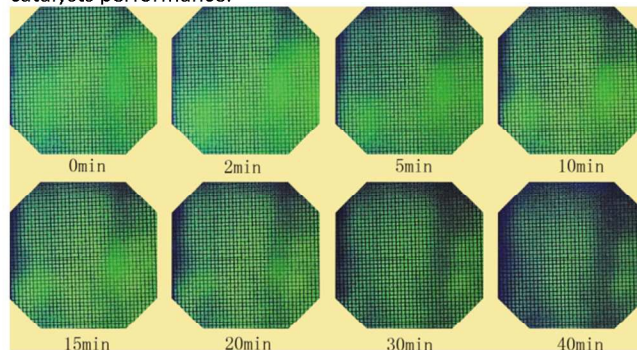


Figure 3. Fluorescence images at certain running times in the PA.

To screen out active catalytic units in PA, optical density (OD) was measured in all react-units. The I^f decrement was determined by OD after a 40 min reaction. The screening method is definitely as follows. The grayscale image of 0 min was subtracted by that of 40 min, then analyzed the sub image by using the Image-Pro Plus software. Through setting area size and the OD threshold, 305 react-units with higher ΔOD values from PA were screened out (accurate values were listed in Table S3). The ΔOD value of these units is directly related to the catalytic efficiency of the catalyst in the units. These ΔOD values were analyzed statistically in Figure 4a, and mainly distributed within the range of 0.10 to 0.18. Nineteen react-units ($\Delta\text{OD} > 0.18$) are much higher in catalytic efficiency, ranked into react-unit 1-19 according to ΔOD . As contrary, a react-unit (noted as 20) with the smallest ΔOD value was screened out as well.

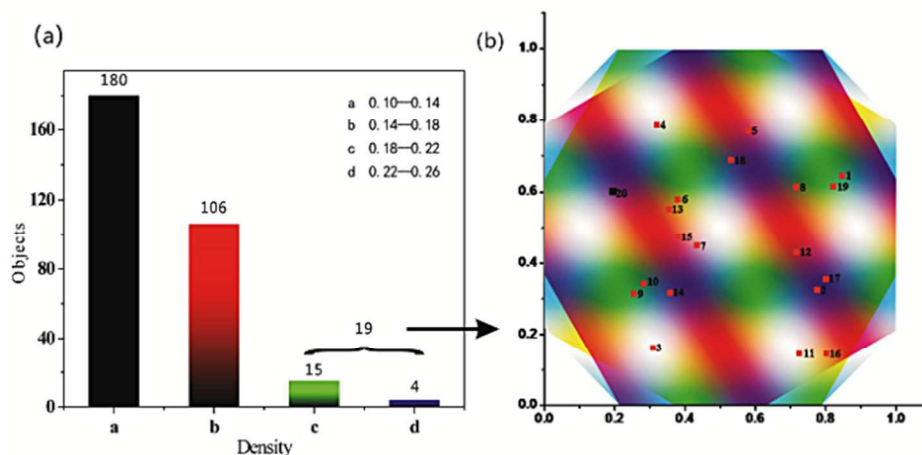


Figure 4. The screening results based on OD measurement in the PA. (a) The ΔOD statistics of 305 react-units. (b) Locations of the selected twenty units (19 highly active units and a low one, 20)

The positions of the screened 20 units (Figure 4b) were located in the designed template to ascertain the R_{atom} of selenides. The generally locating method was: took the template's left bottom as the origin of coordinates, corresponded it with the active units position in the actual reaction zone. By locating it on the designed pattern, we ascertain the CMY ($C_1M_1Y_1C_2M_2Y_2$) value in these units, which corresponded to the relative amount of Ni, Cu, Cd, Ce, In, Y in each channel. Then the 6 metals R_{atom} in react-unit were obtained in the following Table S2. Calculated from CMY value, the 6 metals R_{atom} in react-unit 1-20 were obtained in Table S1. The basic distribution of the active catalyst units was symmetrical, which was consistent with the designed symmetry in the template. From Table S1, the primary content of Ce, Cd, Ni was all greater than 0.2, indicating they might account for main contribution to the catalytic activity of the modified TiO_2 .

The catalytic performance of catalysts in react-units was also evaluated by OD changes during the reaction. The OD changes over reaction time of the three best and contrasting one were studied here. Specific changes were depicted in Figure 5. The I^f changes of unit 1 were the most remarkable (the top-left part of Figure 5). And the OD change rates were unit 1 > unit 2 > unit 3 > unit 4. The I^f in these 4 units all weakened gradually with the increase of time, which was consistent with the catalytic reaction processes.

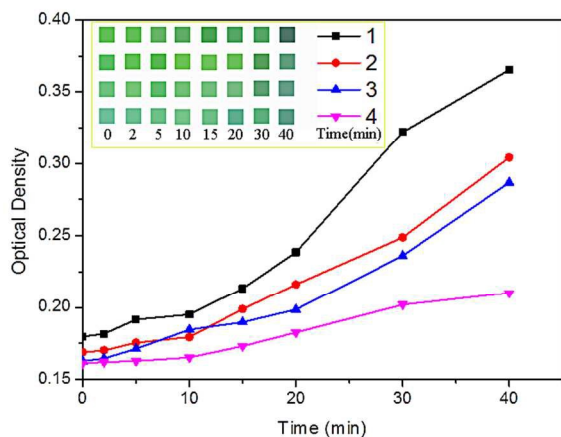


Figure 5. The OD changes of 4 react-units with increasing of reaction time. Unit 1 to 4 were the first three and the last entries listed in Table S1.

The photocatalytic activity of selected $M_6\text{Se}/\text{Ti}$ was also evaluated in ordinary batch experiment. The components of the 4 participant catalysts were $(\text{Ni}_{0.37}\text{Cu}_{0.04}\text{Cd}_{0.28}\text{Ce}_{0.05}\text{In}_{0.15}\text{Y}_{0.11})\text{Se}_x/\text{TiO}_2$, $(\text{Ni}_{0.33}\text{Cu}_{0.33}\text{Cd}_{0.01}\text{Ce}_{0.25}\text{In}_{0.00}\text{Y}_{0.08})\text{Se}_x/\text{TiO}_2$, $(\text{Ni}_{0.02}\text{Cu}_{0.01}\text{Cd}_{0.02}\text{Ce}_{0.48}\text{In}_{0.39}\text{Y}_{0.08})\text{Se}_x/\text{TiO}_2$, $(\text{Ni}_{0.33}\text{Cu}_{0.41}\text{Cd}_{0.02}\text{Ce}_{0.19}\text{In}_{0.04}\text{Y}_{0.01})\text{Se}_x/\text{TiO}_2$ for unit 1 to 4, respectively. The reaction results (Figure S5) showed that within 1 h reaction, degradation efficiency was unit 1 > unit 2 > unit 3 > unit 4. Detailedly, the degradation efficiencies were 93.1%, 89.8%, 87.2% and 42.7%, respectively. The results were in agreement with that from HTS method.

As a conclusion, in this work, a HTS experimentation based on FI was established and implemented to evaluate the photocatalytic performance of selenide-modified nano- TiO_2 . A chip containing numerous independent microreactors was successfully prepared by an UV-lithography method, which realized the control of multiple variables in the same condition. Chemical IJP method is adopted to establish a catalyst library including 1405 $M_6\text{Se}/\text{Ti}$ composite catalysts. The catalyst activity for the degradation reaction was evaluated efficiently by FI technology. By the way, three catalysts with high catalytic efficiency were screened out, $(\text{Ni}_{0.37}\text{Cu}_{0.04}\text{Cd}_{0.28}\text{Ce}_{0.05}\text{In}_{0.15}\text{Y}_{0.11})\text{Se}_x/\text{TiO}_2$, $(\text{Ni}_{0.33}\text{Cu}_{0.33}\text{Cd}_{0.01}\text{Ce}_{0.25}\text{In}_{0.00}\text{Y}_{0.08})\text{Se}_x/\text{TiO}_2$ and $(\text{Ni}_{0.02}\text{Cu}_{0.01}\text{Cd}_{0.02}\text{Ce}_{0.48}\text{In}_{0.39}\text{Y}_{0.08})\text{Se}_x/\text{TiO}_2$. The proposed HTS method avoided the blindness and material-wasting of catalysts optimization and also provided a pathway to explore the extremely-complex catalysts.

ASSOCIATED CONTENT

ACKNOWLEDGMENT

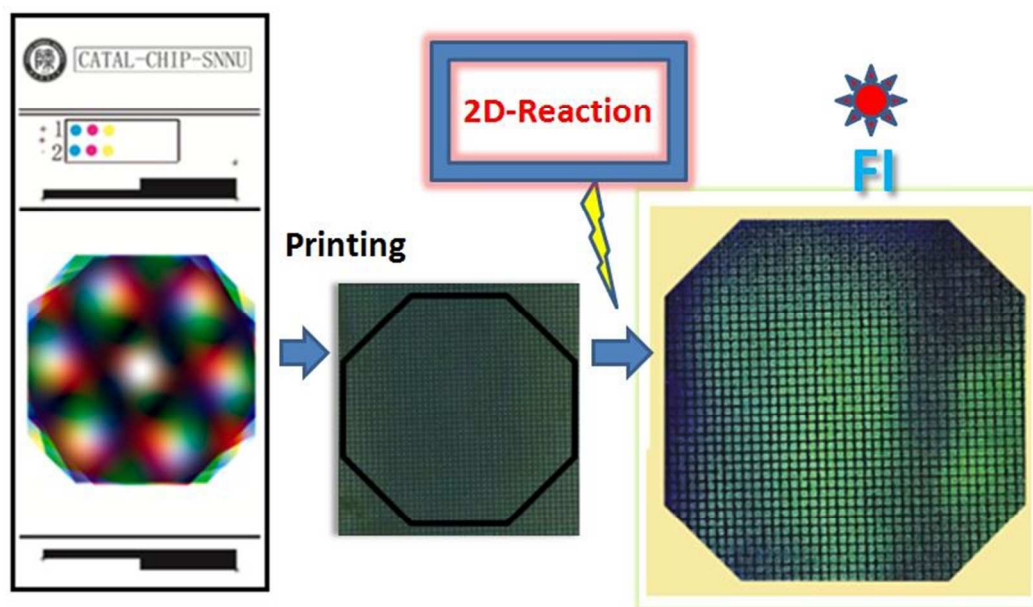
This work is supported by the National Natural Science Foundation of China (No.50309011), the Research Project of Shaanxi Province (2011K17-03-06) and the Scientific Research Foundation for the Returned Overseas Chinese Scholars (08501041585).

REFERENCES

1. Z. Zou, Y. Liu, H. Li, Y. Liao and C. Xie, *Journal of combinatorial chemistry*, 2010, **12**, 363-369.
2. M. Ni, M. K. Leung, D. Y. Leung and K. Sumathy, *Renewable and Sustainable Energy Reviews*, 2007, **11**, 401-425.
3. J. Chen, M. Yao and X. Wang, *Journal of Nanoparticle Research*, 2008, **10**, 163-171.
4. X. Cui, Z. Li, Y. Yang, W. Zhang and Q. Wang, *Electroanalysis*, 2008, **20**, 970-975.
5. D. Chu, Y. Hou, J. He, M. Xu, Y. Wang, S. Wang, J. Wang and L. Zha, *Journal of Nanoparticle Research*, 2009, **11**, 1805-1809.

6. Y. Liu, J. Lee, Y. Zhao, M. Zhang, L. Wang and Q. Duan, *Desalination and Water Treatment*, 2014, 1-7.
7. V. Subramanian, E. Wolf and P. V. Kamat, *The Journal of Physical Chemistry B*, 2001, **105**, 11439-11446.
8. A. Di Paola, E. García-López, G. Marci and L. Palmisano, *Journal of Hazardous materials*, 2012, **211**, 3-29.
9. X. Hua, Z. Liu, P. G. Bruce and C. P. Grey, *Journal of the American Chemical Society*, 2015.
10. G. Ramakrishna, A. Das and H. N. Ghosh, *Langmuir*, 2004, **20**, 1430-1435.
11. S.-m. Chang and W.-s. Liu, *Applied Catalysis B: Environmental*, 2014, **156**, 466-475.
12. P. Wang, L. Wang, B. Ma, B. Li and Y. Qiu, *The Journal of Physical Chemistry B*, 2006, **110**, 14406-14409.
13. C. Xiang, S. K. Suram, J. A. Haber, D. W. Guevarra, E. Soedarmadji, J. Jin and J. M. Gregoire, *ACS combinatorial science*, 2014, **16**, 47-52.
14. H. Chang, C. Gao, I. Takeuchi, Y. Yoo, J. Wang, P. Schultz, X.-D. Xiang, R. Sharma, M. Downes and T. Venkatesan, *Applied Physics Letters*, 1998, **72**, 2185-2187.
15. K. Yang, J. Bedenbaugh, H. Li, M. Peralta, J. K. Bunn, J. Lauterbach and J. Hatrick-Simpers, *ACS combinatorial science*, 2012, **14**, 372-377.
16. Y. Wu, P. Lazić, G. Hautier, K. Persson and G. Ceder, *Energy & Environmental Science*, 2013, **6**, 157-168.
17. L. J. Heidt and L. Ekstrom, *Journal of the American Chemical Society*, 1957, **79**, 1260-1261.
18. M. J. van Dongen, J. Uppenberg, S. Svensson, T. Lundbäck, T. Åkerud, M. Wikström and J. Schultz, *Journal of the American Chemical Society*, 2002, **124**, 11874-11880.
19. B. Weidenhof, M. Reiser, K. Stowe, W. Maier, M. Kim, J. Azurdiá, E. Gulari, E. Seker, A. Barks and R. Laine, *Journal of the American Chemical Society*, 2009, **131**, 9207-9219.
20. A. B. Shapiro, S. Livchak, N. Gao, J. Whiteaker, J. Thresher, H. Jahić, J. Huang and R.-F. Gu, *Journal of biomolecular screening*, 2012, **17**, 327-338.
21. R. P. Hertzberg and A. J. Pope, *Current opinion in chemical biology*, 2000, **4**, 445-451.
22. N. Na, S. Zhang, X. Wang and X. Zhang, *Analytical chemistry*, 2009, **81**, 2092-2097.
23. J. M. Sohn, K. S. Oh and S. I. Woo, *Korean Journal of Chemical Engineering*, 2004, **21**, 123-125.
24. D. Zhao, C. Chen, Y. Wang, H. Ji, W. Ma, L. Zang and J. Zhao, *The Journal of Physical Chemistry C*, 2008, **112**, 5993-6001.
25. J. L. Chin-hsin, J. Olsen, D. R. Sounders and J. H. Wang, *Journal of The Electrochemical Society*, 1981, **128**, 1224-1228.
26. Y. Li, S. Luo, L. Yang, C. Liu, Y. Chen and D. Meng, *Electrochimica Acta*, 2012, **83**, 394-401.
27. W. Shi, J. Shi, S. Yu and P. Liu, *Applied Catalysis B: Environmental*, 2013, **138**, 184-190.
28. C. Wu, C. Szymanski, Z. Cain and J. McNeill, *Journal of the American Chemical Society*, 2007, **129**, 12904-12905.
29. J. P. Lee and M. M. Sung, *Journal of the American Chemical Society*, 2004, **126**, 28-29.
30. J. Liu, D. Song, G. Zong, P. Yin, X. Zhang, Z. Xu, L. Du, C. Liu and L. Wang, *Journal of Micromechanics and Microengineering*, 2014, **24**, 035009.
31. Z. Zheng, O. Azzaroni, F. Zhou and W. T. Huck, *Journal of the American Chemical Society*, 2006, **128**, 7730-7731.
32. D. I. Rozkiewicz, W. Brugman, R. M. Kerkhoven, B. J. Ravoo and D. N. Reinhoudt, *Journal of the American Chemical Society*, 2007, **129**, 11593-11599.
33. H. Hu, J. Lee, M. Wang, N. Xu, H. Chen, Q. Duan and L. Wang, *Chemical Engineering Science*, 2015.

Table of Contents artwork



A high-throughput screening (HTS) method based on fluorescence imaging (FI) was built and applied to evaluate catalytic performance of selenides-modified TiO_2 . A catalyst library comprising 1405 catalysts was established by color ink-jet printing technology.